Proc. MCWASP X, 10th Int. Conf. on Modeling of Casting, Welding and Advanced Solidification Processes, Destin (Florida, USA), May 25-30, 2003, D.M. Stefanescu, J.A. Warren, M.R. Jolly & M.J.M. Krane (eds.), The Minerals, Metals & Materials Society, Warrendale, Pennsylvania, USA, pp. 361-368, 2003

APPLICATION OF THE ARBITRARY EULERIAN LAGRANGIAN FINITE ELEMENT FORMULATION TO THE THERMOMECHANICAL SIMULATION OF CASTING PROCESSES, WITH FOCUS ON PIPE SHRINKAGE PREDICTION

Michel Bellet[1], Victor Fachinotti[1], Olivier Jaouen[2],
Sophie de la Chapelle[3], Isabelle Poitrault[4], Benoît Lusson[5]

[1] Ecole des Mines de Paris, Centre de Mise en Forme des Matériaux (CEMEF), UMR CNRS 7635, BP 207, 06904 Sophia Antipolis, France.
[2] Transvalor S.A., Parc de Haute Technologie, Sophia Antipolis, 694 avenue du Dr. Maurice Donat, 06255 Mougins Cedex, France
[3] Science et Computer Consultants, Parc Giron, 8 rue de la Richelandière, 42100 Saint-Etienne, France
[4] Industeel, Centre de Recherche des Matériaux, 56 rue Clemenceau, BP 56, 71202 Le Creusot, France
[5] Aubert&Duval Holding, , Parc Technologique La Pardieu 6, rue Condorcet, 63063 Clermont-Ferrand Cedex1, France

Abstract

The Arbitrary Lagrangian-Eulerian formulation (ALE) has become an indispensable component of finite element thermomechanical computations of casting processes. As it is an intermediate formulation between the Lagrangian formulation (material convected mesh) and the Eulerian one (fixed mesh), it allows the *simultaneous* computation of important phenomena:

- Deformation and stresses affecting solidified regions, yielding the computation of air gap evolution at part/mold interfaces. In such regions, the formulation is essentially Lagrangian.
- Thermosolutal convection flow in the non solidified regions ; here the ALE formulation tends to a pure Eulerian one (stationary mesh).
- Free surface evolution at top of risers, leading to the prediction of pipe defects (macroshrinkage). In this case the ALE formulation allows the follow up of the free surface.

After a brief reminder of the constitutive equations to be used in thermomechanical modeling of solidification, the mechanical equations are presented and their resolution in the context of FEM-ALE. We insist on the transport analysis, a key-point of ALE, and present a validation of the original scheme that is used here. Finally, we focus on the prediction of pipe shrinkage formation and show two industrial examples.

Introduction

The current state-of-the-art in casting simulation is based on either Eulerian computations, in which the computational grid is fixed, or Lagrangian formulations, in which the computational grid is moving with the material. In the first category, which is by far the most widespread, we find computational models that focus on heat transfer, fluid flow and microstructure prediction. In the second one, we find software aiming at the calculation of distorsions, air gap formation and residual stresses. From the point of view of the end-user of simulation models, this situation has several drawbacks. There is no software able to predict simultaneously the above mentioned solidification features in a single computation. He is forced to make successive simulations, with different modules of a same commercial package, or with different software.

Beyond this practical drawbacks, there are embarrassing situations the engineer can encounter when some of the previous phenomena are coupled. This is the case for instance when the liquid flow in a mushy zone is influenced by the deformation of the solidified material, like in continuous casting, and more generally in all processes where the mushy zone is deformed significantly.
The interest of a more versatile formulation is then obvious. In this paper, we will present the FEM-ALE formulation, which is an intermediate formulation between the two previous one, with the capacity of being fully Eulerian or Lagrangian in certain zones of the computational domain. The Lagrangian character permits a precise description of the evolution of the boundary of the computational domain. This is essential to treat air gap opening, and to predict free surface evolution such as pipe defects. At the same time, a quasi Eulerian formulation allows the computation of thermal convection in liquid pools, associated segregation, feeding flow originated by solidification shrinkage...
The present work is a contribution to the development of the THERCAST® software at Cemef laboratory and Transvalor [Bellet *et al*., 1996 ; Jaouen, 1998; Bellet and Jaouen, 1999]. The main features of this software are:

- Mechanics solved in the part (with inertia and gravity) and in the mold components.
- Between each domain, unilateral contact managed by a penalty technique, including possible Coulomb type friction.
- Velocity-pressure formulation for the weak form of momentum equation. Tetrahedral finite elements. Non linear system solved by Newton-Raphson method. Linear sets of equations solved by preconditioned iterative solvers of minimum residual type.
- Eulerian-Lagrangian formulation for simultaneous modeling of natural convection in liquid pool and of deformation of solidified regions with a follow-up of free surfaces.

1 Constitutive equations for metallic alloys in solidification conditions

In order to overcome the problems raised by the use of a unique elastic-(visco)plastic from liquid to room temperature (ref), it is chosen to distinguish a fluid-type and a solid-type constitutive model, separated by a transition temperature T_C. This temperature can be in the solidification interval ("coherency" temperature), or below the solidus, the elasticity being then neglected for deformations at high temperature. For fluid-like behavior, a thermo-viscoplastic model is used (1). The strain rate tensor is split into viscoplastic and thermal parts. The first one is related to the stress deviator by a non-Newtonian law. The second one includes thermal dilatation and solidification shrinkage. The solid-like behavior is modeled by a thermo-elastic-viscoplastic law (2). Elasticity obeys the Hooke's law. The plastic law includes a threshold and strain-rate sensitivity. In this case, expression (1c) remains valid.

$$\dot{\boldsymbol{\varepsilon}} = \dot{\boldsymbol{\varepsilon}}^{vp} + \dot{\boldsymbol{\varepsilon}}^{th} \qquad \dot{\boldsymbol{\varepsilon}}^{vp} = \frac{1}{2K}\left(\sqrt{3}\dot{\varepsilon}_{eq}\right)^{1-m}\boldsymbol{s} \qquad \dot{\boldsymbol{\varepsilon}}^{th} = \left(\alpha\dot{T} + \frac{1}{3}\dot{g}_s\Delta\varepsilon^{tr}\right)\boldsymbol{I} \quad (1)$$

$$\dot{\boldsymbol{\varepsilon}} = \dot{\boldsymbol{\varepsilon}}^{el} + \dot{\boldsymbol{\varepsilon}}^{vp} + \dot{\boldsymbol{\varepsilon}}^{th} \qquad \dot{\boldsymbol{\varepsilon}}^{el} = \frac{1+\nu}{E}\dot{\boldsymbol{\sigma}} - \frac{\nu}{E}\mathrm{tr}(\dot{\boldsymbol{\sigma}})\boldsymbol{I} \qquad \dot{\boldsymbol{\varepsilon}}^{vp} = \frac{\sqrt{3}}{2\sigma_{eq}}\left\langle\frac{\sigma_{eq} - (\sigma_{00} + H{\varepsilon_{eq}}^{n})}{K\sqrt{3}}\right\rangle^{1/m}\boldsymbol{s} \quad (2)$$

2 Mechanical equilibrium equations and resolution

At any time, in any domain (the solidifying part or the mold components) the mechanical equilibrium is governed by the momentum equation:

$$\nabla.\boldsymbol{\sigma} + \rho\boldsymbol{g} - \rho\boldsymbol{\gamma} = \nabla.\boldsymbol{s} - \nabla p + \rho\boldsymbol{g} - \rho\boldsymbol{\gamma} = 0 \quad (3)$$

where $\boldsymbol{g}$ and $\boldsymbol{\gamma}$ respectively denote the gravity and acceleration vector (negligible in molds). The treatment of mechanical boundary conditions is not presented here, refer to [Bellet *et al*, 2002]. Using the velocity-pressure formulation, the weak form of (3) is:

$$\begin{cases} \forall \boldsymbol{v}^* & \int_\Omega \boldsymbol{s} : \dot{\boldsymbol{\varepsilon}}^* dV - \int_\Omega p \nabla . \boldsymbol{v}^* dV - \int_{\partial\Omega} \boldsymbol{T} . \boldsymbol{v}^* dS - \int_\Omega \rho \boldsymbol{g} . \boldsymbol{v}^* dV + \int_\Omega \rho \boldsymbol{\gamma} . \boldsymbol{v}^* dV = 0 \\ \forall p^* & \int_\Omega p^* \operatorname{tr} \dot{\boldsymbol{\varepsilon}}^{vp} dV = 0 \end{cases} \tag{4}$$

The form of the term integrated in the second equation changes according to the local state of the alloy (*i.e.* the local temperature):

$$\text{solid-like (elastic-viscopl)} : \operatorname{tr} \dot{\boldsymbol{\varepsilon}}^{vp} = \operatorname{tr} \dot{\boldsymbol{\varepsilon}} - \operatorname{tr} \dot{\boldsymbol{\varepsilon}}^{el} - \operatorname{tr} \dot{\boldsymbol{\varepsilon}}^{th} = \nabla . \boldsymbol{v} + \frac{3(1-2\nu)}{E} \dot{p} - 3\alpha \dot{T} - \dot{g}_s \Delta \varepsilon^{tr} \tag{5}$$

$$\text{liquid-like (viscoplastic)} : \quad \operatorname{tr} \dot{\boldsymbol{\varepsilon}}^{vp} = \operatorname{tr} \dot{\boldsymbol{\varepsilon}} - \operatorname{tr} \dot{\boldsymbol{\varepsilon}}^{th} = \nabla . \boldsymbol{v} - 3\alpha \dot{T} - \dot{g}_s \Delta \varepsilon^{tr} \tag{6}$$

Accordingly, the stress deviator $\boldsymbol{s}$ in (4a) results either from an elastic-viscoplastic constitutive equation, or from a viscoplastic or Newtonian law. Given the configuration occupied by the cast part at time t, equations (4) are solved for $(\boldsymbol{v}, p)^t$, velocity and pressure field at time t. In these equations, $\dot{T}$ and $\dot{g}_s$ are provided by the thermal resolution and the time derivatives of pressure and velocity are approached by implicit Euler backward finite difference schemes:

$$\dot{p}^t = \frac{1}{\Delta t}(p^t - p^{t-\Delta t}) \qquad \boldsymbol{\gamma}^t = \frac{1}{\Delta t}(\boldsymbol{v}^t - \boldsymbol{v}^{t-\Delta t}) \tag{7}$$

After resolution, the configuration updating is defined by:

$$\boldsymbol{x}^{t+\Delta t} = \boldsymbol{x}^t + \Delta t \boldsymbol{v}^t + \frac{\Delta t^2}{2} \boldsymbol{\gamma}^t \tag{8}$$

The finite element mesh is composed of linear tetrahedra. The mini-element bubble-type P1+/P1 element is used [Arnold *et al*., 1984; Fortin and Fortin, 1985]. The velocity field is linear continuous, including additional degrees of freedom at the center of the element (bubble formulation), and the pressure field is linear continuous. The equilibrium equation (4a) is then projected onto the P1 space and onto the "bubble" space (see [Jaouen, 1998 ; Bellet and Jaouen, 1999]). After elimination of the bubble degrees of freedom, this leads to the resolution of a non linear equation whose unknowns are the nodal pressures and velocities. This set of equations is solved by a Newton-Raphson method. At each iteration, the resolution of the set of linearized equations is performed by an iterative solver with block diagonal preconditioning. Such a mini-element formulation provides a perfect compatibility between the treatment of an elastic-viscoplastic medium and a pure viscoplastic or Newtonian medium. Therefore, it allows to treat simultaneously the solidified zones and the liquid or mushy pools of a casting. The above mentioned choice between the two constitutive models is done when assembling each finite element, depending on the central temperature. If it exceeds the critical temperature T_C, then the whole element is considered viscoplastic, otherwise it is elastic-viscoplastic.

3 ALE formulation

In solidification analysis Lagrangian formulations are not satisfying because they lead to mesh degeneracy in liquid pools. At the same time, purely Eulerian schemes cannot provide enough precision for free surface evolution: the location of the physical boundary of the part by a front tracking algorithm is irrelevant when dealing with air gap opening for instance. This motivates the development of Lagrangian-Eulerian formulations such as the one presented hereunder.

The basic principle of the ALE method is to separate clearly the mesh velocity field $\boldsymbol{v}_{msh}$ from the material velocity field $\boldsymbol{v}_{mat}$ (previously denoted $\boldsymbol{v}$ and coming from the resolution of (4)). Hence the ALE method is between the Lagrangian method ($\boldsymbol{v}_{msh} = \boldsymbol{v}_{mat}$) and the Eulerian one ($\boldsymbol{v}_{msh} = 0$). There are two main problems to be solved: the computation of the mesh velocity field and the consideration of the velocity difference $\boldsymbol{v}_{mat} - \boldsymbol{v}_{msh}$ in the energy and momentum equations [Donea, 1977 ; Huerta, 1988 ; Baaijens, 1993 ; Chenot and Bellet, 1995].

3.1 Computation of mesh velocity

The computation of $\boldsymbol{v}_{msh}$ consists in regularizing the position of nodes in order to minimize the deformation of the elements. Given Δt, the mesh velocity is defined by the relation

$$\boldsymbol{x}^{t+\Delta t} = \boldsymbol{x}^{t} + \Delta t\, \boldsymbol{v}_{msh} \tag{9}$$

The new nodal positions $\boldsymbol{x}^{t+\Delta t}$ are determined by an iterative procedure which aims at positioning each node at the center of gravity of the set of its neighbors. This is done under the constraint of material flux conservation through the surface:

$$\boldsymbol{v}_{msh}.\boldsymbol{n} = \boldsymbol{v}_{mat}.\boldsymbol{n} \tag{10}$$

where $\boldsymbol{n}$ is the outward unit normal. This constraint is enforced by a local penalty technique. In (10) we use the so-called "consistent" normal vectors, which are such that any tangential nodal velocity (*i.e.* a velocity which is orthogonal to the consistent normal vector) provides a null contribution to the flux through the discretized surface. For linear elements, the consistent normal vector at each surface node is defined by the average of the normals of the surrounding facets weighted by their surface [Bellet, 2001].

3.2 Transport of the variables

Knowing the mesh velocity, the updating of any nodal field B is done as follows.

$$B(x^{t+\Delta t}, t+\Delta t) = B(x^{t}, t) + \frac{d_g B}{dt}\Delta t \tag{11}$$

where the time derivative of B with respect to the grid can be expressed as follows:

$$\frac{d_g B}{dt} = \frac{dB}{dt} - (\boldsymbol{v}_{mat} - \boldsymbol{v}_{msh}).\nabla B \tag{12}$$

The concept of upwind derivative is introduced in (12), which is considered at each node and in which the nodal gradient of B is expressed in the element in the direction of $\boldsymbol{v}_{msh} - \boldsymbol{v}_{mat}$ (fig. 1). The update of B, as defined by (11) has probed to be accurate only if Δt remains small enough,

$$\Delta t \le \Delta t_c = \min_e \frac{h^e}{\left|\boldsymbol{v}^e_{mat} - \boldsymbol{v}^e_{msh}\right|} \tag{13}$$

h^e being the size of element e. In this work, this restriction is circumvented by carrying out the transport during $[t,t+\Delta t]$ in n sub-steps $[t,t_1]$, $[t_1,t_2]$,…, $[t_{n-1},t+\Delta t]$, being $t_i = t+i\Delta t_c$. In practice, n should not exceed 6 in order to keep a satisfactory accuracy.

3.2.1 Validation of transport scheme

We will use the widely-studied problem of natural convection in a Boussinesq fluid contained in a square cavity [De Vahl Davis and Jones, 1983] as a benchmark for validating the present ALE scheme. Fig. 2 shows the finite element mesh (3153 nodes, 8893 linear tetrahedra, one layer of elements in the third direction), as well as the stationary concentration fields for Raleigh number Ra equal to 10^3 and 10^4; the Prandtl number is set to 0.71 in both cases. Present

results are in good agreement with the benchmark solution, as shown in Table 1. Regarding time discretization, a constant time step Δt=0.25 s was adopted for both cases. Condition (13) is satisfied a priori for Ra=10^3 ($\Delta t/\Delta t_{max}$=1.58), while four substeps were taken ($\Delta t/\Delta t_{max}$=3.38) in case Ra=10^4 preserving a proper accuracy.

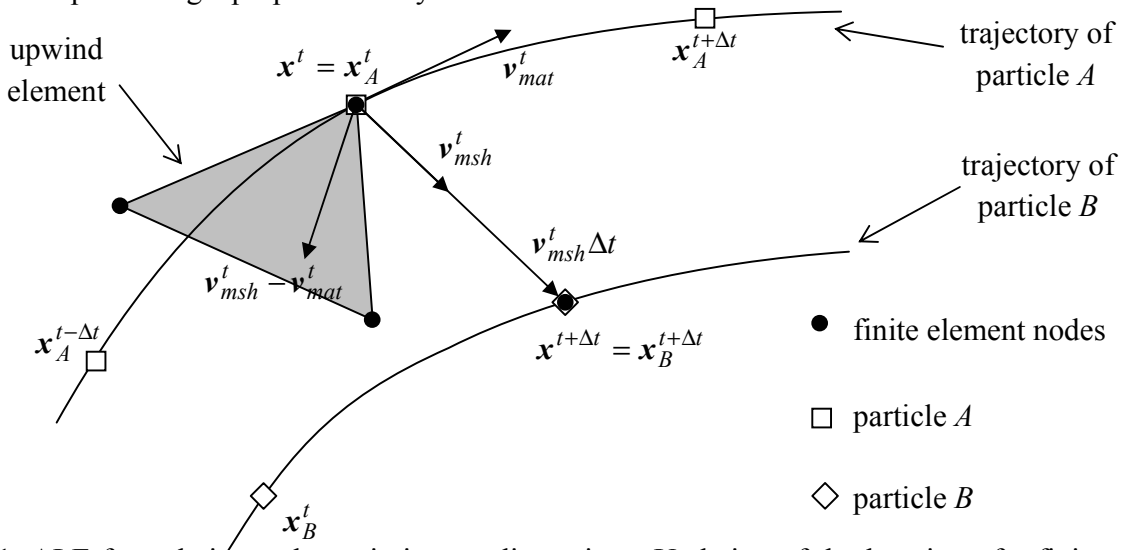

Figure 1. ALE formulation: schematic in two dimensions. Updating of the location of a finite element node and subsequent identification of the upwind element.

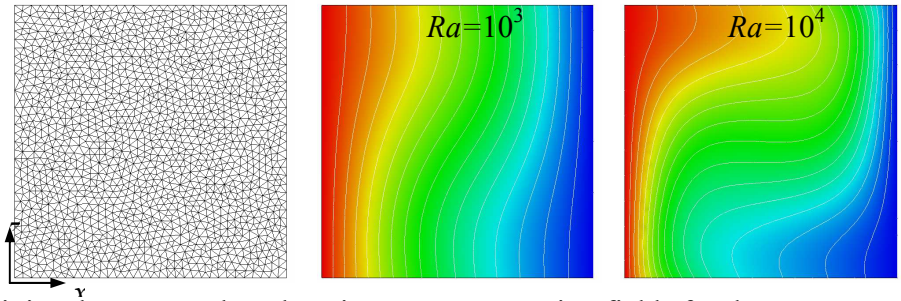

Figure 2: Finite element mesh and stationary concentration fields for the square cavity test.

	Ra =10^3		Ra =10^4	
	De Vahl Davies & Jones	Present solution	De Vahl Davies & Jones	Present solution
max(v_x)	3.649	3.634	16.178	16.099
z	0.813	0.811	0.823	0.814
max(v_z)	3.697	3.669	19.617	19.413
x	0.178	0.183	0.119	0.108

Table 1: Maximum values of velocity components for the square cavity test.

3.3 Lagrangian and Eulerian-Lagrangian zones

Regarding now the global treatment of a casting, the idea consists in defining the solidified regions as Lagrangian (convected mesh) and the liquid or mushy ones as Eulerian-Lagrangian (regularized mesh under the constraint (26)). Therefore each node is affected to one of the two classes, according to the following rule, as illustrated in fig. 3. Each node belonging at least to one solid-like element is treated as Lagrangian. All other nodes, which then belong to liquid-like elements only, are treated as Eulerian-Lagrangian. This ALE formulation prevents the mesh from degenerating when fluid motion occurs in the casting, due to thermal convection.

Also it allows the mesh boundary to follow the evolution of the free surface of the remaining liquid pool and then to model air gap and pipe formation.

4 Applications

4.1 Casting of very large parts: magnet components

The parts studied here are elements of very large electro-magnets, used in electron accelerators. Each magnet is composed of two identical parts, which are cast by the foundry of Industeel. These parts are very specific by their weight (125 tons each), their dimensions (2.5 x 7.0 x 1.0 m) and the steel grade. Their particular magnetic properties require the use of a carbon-free steel, developed by the research center of Industeel.

Preliminary computations have been done, only using the heat transfer module of the THERCAST® software. This has permitted a fast determination of the shape and the volume of the riser, as well as of the different elements of the mold. The geometry that has been finally determined, using a single central riser, is shown schematically in fig. 2. In a second step, a full thermomechanical computation has been done in order to precisely determine the shape of the primary shrinkage defect in the riser. This defect comes from local shrinkage at solidification front, which initiates liquid flow to compensate these local volume contractions. This results in the macroscopic collapse of the free surface of the casting during its cooling down. The present configuration includes seven subdomains: the cast part and six mold components, which have been meshed separately, without any interface constraint. Using symmetry conditions, half of the casting has been calculated. The part has approximately 120 000 elements (average mesh size 0.1 m) and the mold subdomains 373 000. In a first approach, the mold has been considered as non deformable. The complete cooling of the part has been simulated, until room temperature (actual process time 333h, simulation time: 8 days on a IBM44-P270 machine).

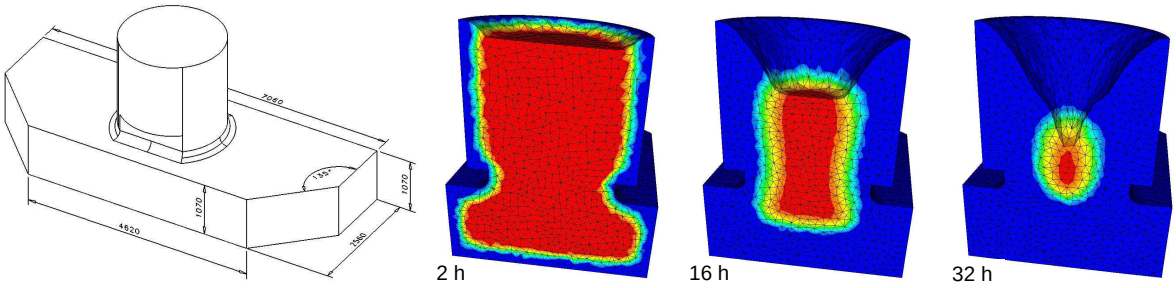

Figure 2. Part geometry. Evolution of primary shrinkage, with liquid fraction distribution.

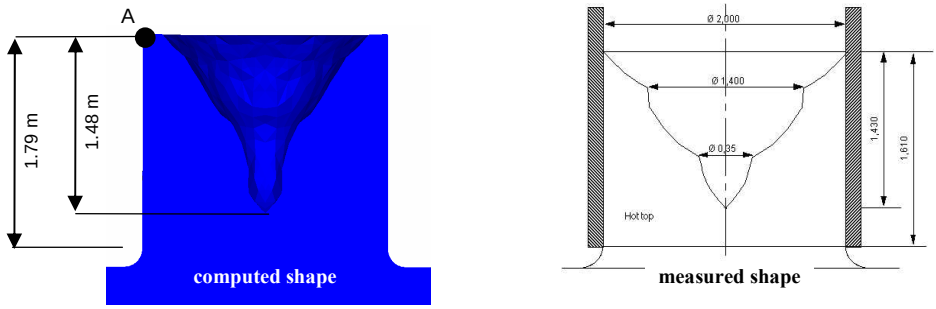

Figure 3. Comparison computation/measurement of pipe shape. Longitudinal section.

In fig. 2, the shape of the pipe in the riser is shown for different process times: 2, 16, and 32 h, close to the end of solidification (36 h). Thanks to ALE formulation, the mesh follows the evolution of the free surface and remains regular throughout the computational domain.

However, twenty complete remeshings have been needed in order to avoid mesh degeneracy along the pipe surface. It can be noted that when a liquid free surface is still present, it remains perfectly horizontal. This is a consequence of the clear distinction between liquid-type and solid-type constitutive equations. The final shape of the pipe calculated by the simulation is given in fig. 3a. There is a reasonably good agreement with the profile experimentally measured on two real (fig. 3b). The v-shape is globally well simulated. The predicted maximum depth is 1.48 m, versus 1.43 m measured, which is excellent. However the precise shape of the pipe is not obtained, partly because of a limited knowledge of rheological data in mushy state.

4.2 Ingot casting

Fig. 4 shows the geometry of octogonal ingots (3.3 tons) made of special steels cast by Aubert&Duval Holding. Their specific shape permits an oriented solidification. A full thermomechanical computation has been done in order to determine the shape of the primary shrinkage defect in the riser and the air gap between the ingot and the mold.

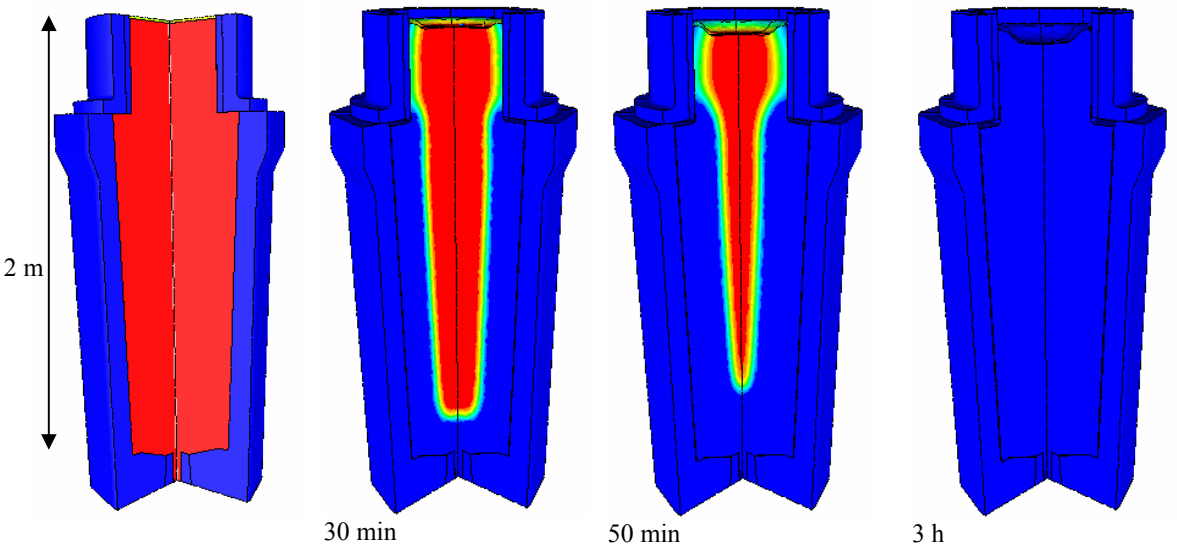

Figure 4. Geometry of the ingot (6/8 of the geometry is represented). Evolution of the primary shrinkage with the liquid fraction evolution for the metal in the molds.

The configuration includes six subdomains: the cast part and five mold components, which have been meshed separately, without any interface constraint. Using symmetry conditions, 1/8 of the casting has been calculated. The part has approximately 40000 elements (average mesh size 0.02 m) and the mold subdomains 97000. In a first approach, the mold has been considered as non deformable. The cooling has been simulated until complete solidification of the ingot (actual process time 3 h, simulation time required : 60 h on a P4-1GHz machine). In fig. 4, the shape of the primary shrinkage is shown for different process times: 30 mn , 50 mn and 3 h. As for the magnet components, the ALE formulation allows the mesh to follow the evolution of the free surface. When a liquid free surface is still present, it remains perfectly horizontal. The depth of the primary shrinkage is in good agreement with the measured size (6.5 cm computed versus ~8 cm measured). In fig.5, it can be seen that a large air gap appears at the top of the ingot under the mold of the riser. Its evolution can be seen at 3 process times (1 mn, 50 mn and 3 h). The calculated size of the air gap is in good agreement with the measured one (2.5 cm for the simulation versus ~3 cm measured).

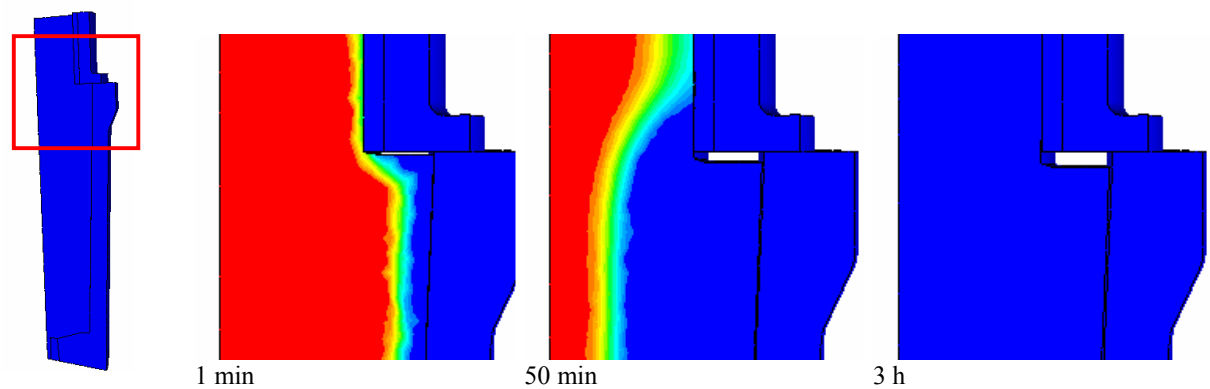

Figure 5. Air gap evolution with liquid fraction distribution.

Conclusion

As a conclusion, the capacity of the FEM-ALE method has been demonstrated for thermomechanical simulations of solidification processes, allowing the concurrent simulation of the formation of air gaps and pipe shrinkage defects.

Acknowledgement

This work has been supported by the French Ministry of Industry, the French Technical Center of Casting Industries (CTIF) and the companies Arcelor-Irsid, Ascometal, Fonderie Atlantique Industrie, Aubert&Duval Holding, Erasteel, Industeel and PSA.

References

Baaijens F.P.T., An U-ALE formulation of 3-D unsteady viscoelastic flow, Int. J. numer. methods Engrg., 36 (1993) 1115-43.

Bellet, M., Decultieux, F., Ménaï, M., Bay, F., Levaillant, C., Chenot, J.L., Schmidt, P. and Svensson, I.L. (1996), Thermomechanics of the cooling stage in casting processes: 3D finite element analysis and experimental validation, *Metall. Mater. Trans. B*, Vol. 27, 81-100.

Bellet, M. and Jaouen, O. (1999), Finite element approach of thermomechanics of solidification processes, *Proc. Int. Conf. On Cutting Edge of Computer Simulation of Solidification and Casting, Osaka*, I. Ohnaka and H. Yasuda (eds.), The Iron and Steel Institute of Japan, 173-190.

Bellet, M. (2001), Implementation of surface tension with wall adhesion effects in a three-dimensional finite element model for fluid flow, *Comm. Num. Meth. Engng*, Vol. 17, 563-579.

M. Bellet, O. Jaouen, I. Poitrault, An ALE-FEM Approach to the Thermomechanics of Solidification Processes with Application to the Prediction of Pipe Shrinkage, submitted to Int. J. Num. Meth. for Heat & Fluid Flow, 2002.

Chenot, J.-L. and Bellet, M. (1995), The ALE method for the numerical simulation of material forming processes, *Proc. Numiform'95, 5th Int. Conf. on Numerical Methods in Industrial Forming Processes, Ithaca*, S.-F. Shen and P.R. Dawson (eds.), Balkema, Rotterdam, 39-48.

Donea J., Fasoli-Stella P., Giuliani S., Lagrangian and Eulerian finite element techniques for transient fluid-structure interaction problems, 4th SMIRT conf., San Francisco, 1977, B1/2.

Fortin, M. and Fortin, A. (1985), Experiments with several elements for viscous incompressible flows, *Int. J. Num. Meth. Fluids*, Vol. 5, 911-928.

Inoue, T. and Ju, D.Y. (1992), Simulation of solidification and viscoplastic stresses during vertical semi-continuous direct chill casting of aluminium alloy, *Int. J. Plasticity*, Vol. 8, 161-183.

Huerta A. and Casadei F., New ALE applications in non-linear fast-transient solid dynamics, Eng. Comput., 11 (1994) 317-345.

Jaouen, O. (1998), *Modélisation tridimensionnelle par éléments finis pour l'analyse thermomécanique du refroidissement des pièces coulées (Three-dimensional finite element modelling for the thermomechanical analysis of the cooling of castings)*, PhD Thesis (in french), Ecole des Mines de Paris.